

## Grain Boundary Segregation: the New Sprouts

*Bokstein Boris, Itckovich Alexei, Pokhvisnev Yury, Rodin Alexei*

Department of physical chemistry. National University of Science and Technology – Moscow  
Institute of Steel and Alloys. Leninsky Pr. 4, 119049 Moscow. Russia.

Corresponding author: bokstein@mail.ru

**Keywords:** grain boundary segregation, atomic interaction, atomic complexes, thermodynamic and atomic models, molecular dynamics simulation.

### Abstract

Some aspects of grain boundary segregation (GBS) are discussed. This paper adds two new sprouts. The first is connected with formation of the atomic complexes in boundary region and their effect on grain boundary diffusion (GBD). The second – with a nonhomogeneity of energy distribution between boundary sites.

### Introduction

Grain boundary (GB) is a transition region between two identical and one-phase crystals (grains) with different crystallographic orientation. Such definition distinguishes clearly GB from other type of interfaces: external surface, interphase boundaries etc. The theory of GBs in solids is described in many monographs and reviews [1-8].

Shortly, effect of segregation can be formulated by the following way: the concentration of the solute  $C_b$  is not equal to its concentration in grain ( $C$ ). The difference can be described by enrichment coefficient  $s$ :

$$s = \frac{C_b}{C}. \quad (1)$$

There are two types of atomic interaction in GBS: interaction of solute atoms with GB – segregation effect and excess interaction (comparing with interaction in the bulk) between solute atoms with formation of atomic complexes.

The introduction contains a short review of different models of segregation effect description.

It is proposed usually that GB is a non-equilibrium defect of crystal. If non-equilibrium of GB is defined only by geometric restrictions, the GB is in equilibrium with grains, which it separates, and it can be described by thermodynamic methods [9], such as Gibbs method of surface excesses [10]. According to this method two main surface excess (adsorption or segregation -  $\Gamma$  and surface tension -  $\sigma$ ) are connected at constant temperature and pressure by the following equation:

$$d\sigma = -\sum \Gamma_i d\mu_i, \quad (2)$$

where  $\mu_i$  is chemical potential of  $i$ -component of solution.



The segregation isotherm can be obtained as a result of quasi-chemical reaction exchange between solvent atoms ( $A$ ) in GB ( $b$ ) and solute ( $B$ ) in the bulk



The equilibrium constant can be written as

$$b = \frac{X_{Bb}(1-X_B)}{X_B(1-X_{Bb})} \quad \text{or} \quad X_{Bb} = \frac{bX_B}{1-X_B+bX_B} \quad (4)$$

The Gibbs approach was further developed taking into account different segregation isotherms such as for: the effect of saturation [11-13]; the GB inhomogeneity [14]; the nonideality of GB solutions [15]; the limited number of segregation sites.

### Thermodynamic modeling of the atomic complexes formation

The main idea is that atomic interaction in GBs and GBS leads to the formation in GB solution the atomic complexes with atomic configuration and chemical bonds very closed to the phase in grain (Guttman [16], Briant [17] and others).

29 years ago, at DIMAT-92 J. Bernardini and P. Gas presented the talk “Diffusion and 2D-chemistry in Grain Boundaries”[18]. Two main conclusions of their presentation: ”strong solute segregation decreases GBD coefficients and peculiarities of GBD in solid solutions may be well described assuming the formation of 2D-phases in segregated GBS”. These conclusions more or less correspond to our today feeling of GBS effect on GBD.

In a set of papers [19-21] two types of complexes were considered:  $A_mB_n$  (mainly,  $AB$ ) type for the systems with restricted solubility and intermediate phases and  $B_2$  type for the systems without intermediate phases (Fig. 1).

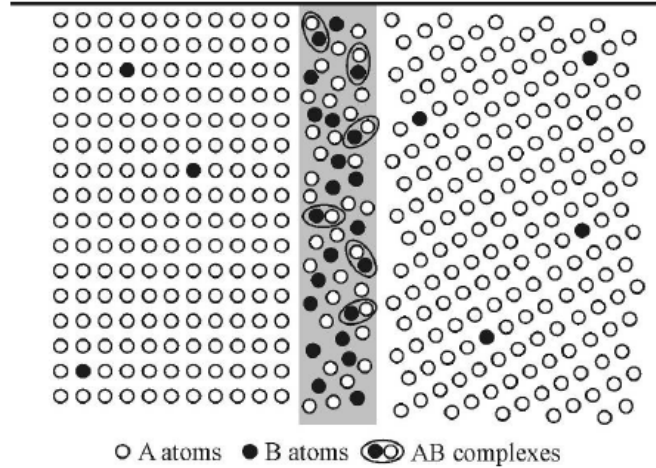


Fig. 1. Schematic illustration of complex formation model. Complexes  $AB$  exist in GB only

So now GB solution consists free atoms  $A$ ,  $B$  and complexes. Schematic illustration of  $AB$  complexes formation is shown on Fig. 1. In the case of the complexes formation the equilibrium between bulk and GB sets up not only due to the simple exchange of the atoms between GB and the bulk but also due to the chemical interaction of GB atoms.  $K$  is the equilibrium constant for the reaction of the complexes formation, if in parallel with exchange reaction (Eq. 3) we add the reaction of complex formation:



In general case this constant can be written as:

$$K = \frac{X_{comp-b}}{X_{Ab}^m X_{Bb}^n} \quad (5)$$

The more  $K$ , the more is complexes concentration (Fig. 2).

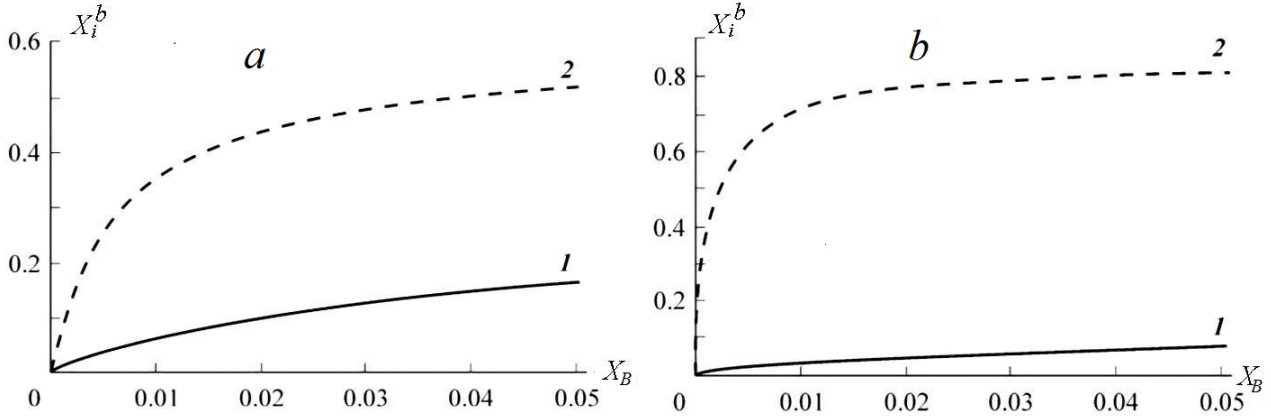


Fig. 2. The isotherm, describing the concentration of complexes  $AB$  (2) and free  $B$  atoms (1) in GB, in dependence on volume concentration of  $B$  ( $a - K = 10$ ,  $b - K = 100$ )

With assumption that the complexes are immobile in GB, but the atoms from the complexes are involved in the leakage to the bulk, the analytical solution of the diffusion problem was obtained for different type of complexes.

This effect leads to decreasing of diffusion flux along the GB (Fig. 3). Consequently, the complexes formation decreases the measured GB self- and heterodiffusion coefficients. This effect can be very strong, if  $K$  is high.

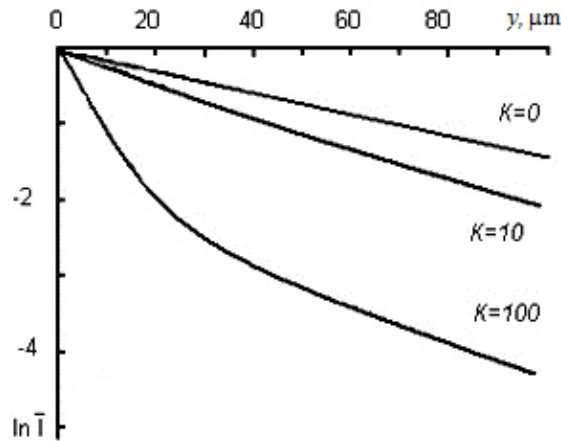


Fig. 3. Calculated profiles of GBD with regards to  $AB$  complexes formation at different  $K$ -values ( $b = 10$ )

### Computer modeling of the complexes formation and their effect on GBD [22-24]

The initial model of the Cu bycrystal with the  $\langle 100 \rangle \Sigma 5$  symmetric GB was created by bringing together two single grains tilted with respect to each other by  $18.43^\circ$ . If the atomic separation was less than 0.05 nm one of the atoms was removed. The simulation cell contained 269640 atoms and had the periodic boundary conditions in all directions and therefore, contained two identical GBS. After a preliminary energy minimization at  $T = 0$ , the model was annealed at 1000 K during 100 ns,

cooled down to 0 K after which the final energy minimization was performed. The GB energy for the final atomic configuration was  $\gamma = 947.7 \text{ mJ/m}^2$ .

The general view of the model is shown on Fig. 4, a scheme of atomic disposition in GB – on Fig. 5.

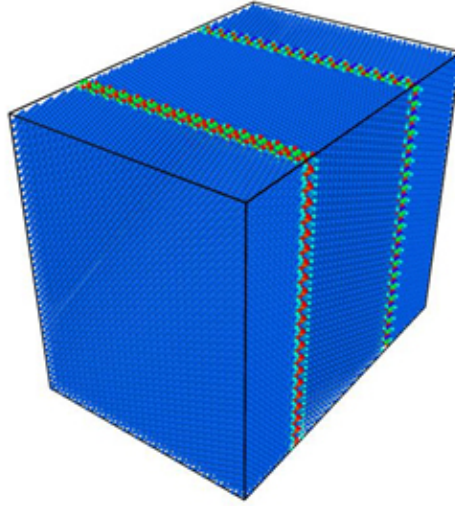


Fig. 4. General view of the model

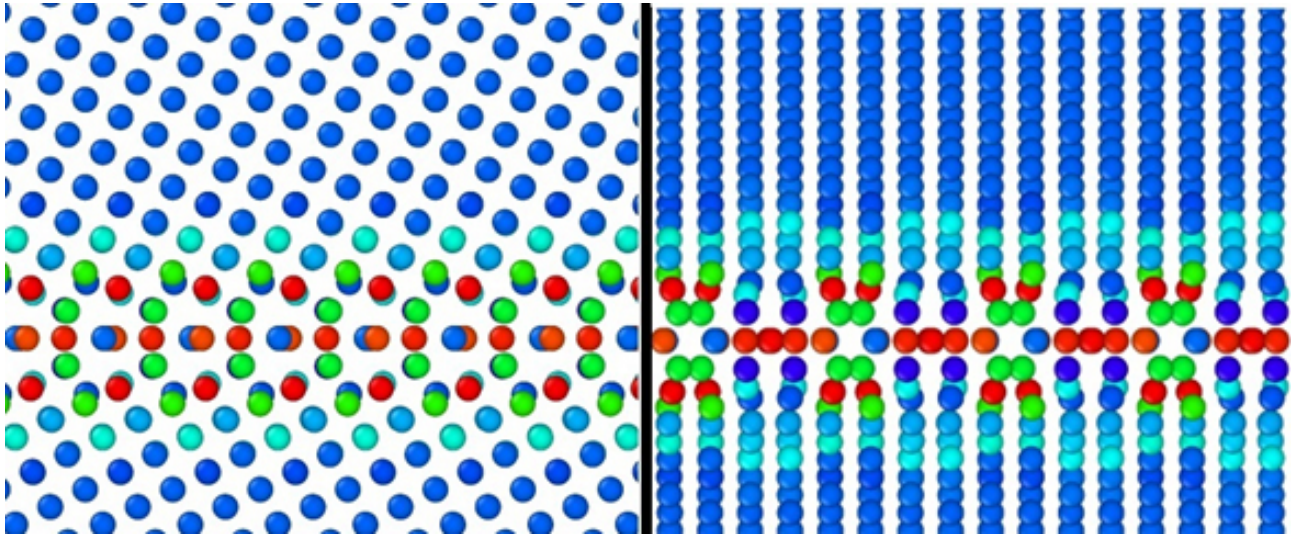


Fig. 5. Scheme of atoms disposition in symmetric GB  $\Sigma 5$  in directions (100) and (010)

### Construction of the semi-empirical potentials for simulation of heterodiffusion

The most popular types of semi-empirical potentials used in molecular dynamics simulations of metal properties are the embedded atom method (EAM) and Finnis-Sinclair (FS) potentials. In contrast to pair potentials these potentials are many-body potentials which allows them to reproduce some important metal properties that pair potentials cannot. In the present study, we employed the FS potential. The total potential energy in this case takes the following form:

$$U = \sum_{i=1}^{N-1} \sum_{j=i+1}^N \phi_{t_i t_j}(r_{ij}) + \sum_{i=1}^N \Phi_{t_i}(\rho_i), \quad (7)$$

where  $t_i$  is the elemental type of atom  $i$ ,  $N$  is the number of atoms in the system,  $r_{ij}$  is the separation between atoms  $i$  and  $j$ ,  $\phi_{t_i t_j}(r)$  is the pairwise potential,  $\Phi_{t_i}(\rho)$  is the embedding energy function and

$$\rho_i = \sum_j \psi_{i,j}(r_{ij}), \quad (8)$$

where  $\psi_{i,j}(r)$  are density functions.

In the present study, the Cu potential was chosen for both the solvent and solute atoms. The cross-function  $\psi_{12}(r)$  was also the same as for the pure elements. Thus the only potential function which we modified was  $\phi_{12}(r)$ .

To control the deviation from ideality we included the partial relative heat of solution, defined as

$$\Delta\bar{H}_2 = \frac{(N_1 + N_2)E_s - N_1E_1^0 - N_2E_2^0}{N_2}, \quad (9)$$

where  $E_s$ ,  $E_1^0$  and  $E_2^0$  are the per atom energies of the solution and pure elements, respectively.

In all cases considered in the present study, we chose the systems with positive deviation from ideality and used  $\Delta\bar{H}_2 = 0.12$  eV/atom as the target value, which approximately corresponds to the value for Fe solutes in Cu.

The potentials were also fit to the desired value of the segregation energy ( $\Delta E_s$ ) which was defined as the difference between the energy of the simulation cell containing only 1 solute atom located at arbitrary site on the GB and the energy of the same simulation cell containing only 1 solute atom located in the bulk (Fig. 6). Finally the potentials were fit to the solute dipole (pair) interaction energy,  $E_p$ , which was defined as the change in the energy associated with bringing together two solute atoms located far away from each other in the bulk phase (Fig. 7).

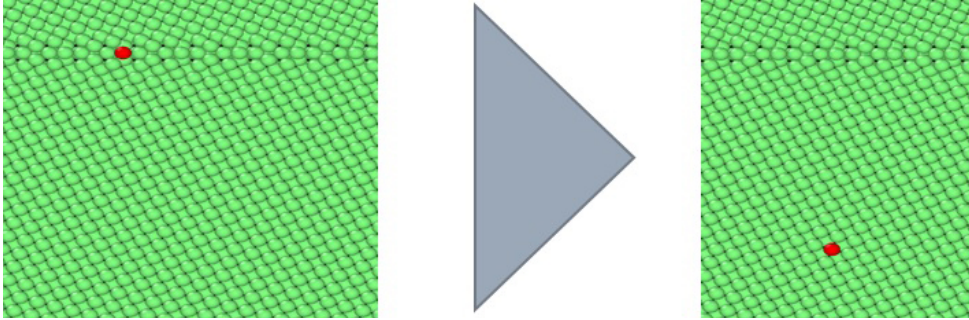


Fig. 6. Scheme of transfer of single atom from bulk to grain boundary (segregation)

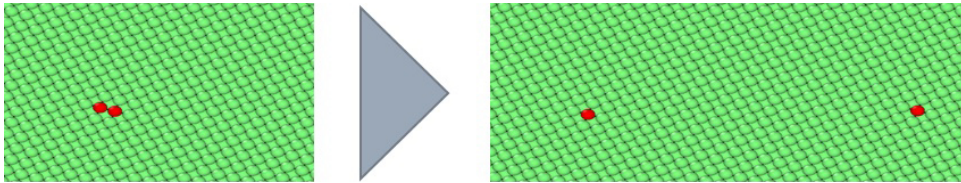


Fig. 7. Scheme of pair formation in grain boundary.

The properties of the developed potentials are provided in Table 1. They all provide about the same value for the partial relative heat of solution ( $\Delta\bar{H}_2$ ) but rather different combinations of the dipole (pair) interaction energy and the energy of segregation.

Table 1. Material properties obtained with the developed semi-empirical potentials

Potential	$\Delta\bar{H}_2$ , (eV/atom)	$\Delta E_p$ , (eV/atom)	$\Delta E_s$ , (eV/atom)
#1	0.13	-0.059	0.008
#2	0.13	-0.199	0.006
#3	0.10	-0.497	0.014
#4	0.14	-0.063	0.478
#5	0.13	-0.285	0.463

It is important to emphasize that for all potentials  $\Delta E_s > 0$ , what corresponds to desegregation.

In order to simulate the heterodiffusion we replace some Cu atoms by the atoms different from others (marked or  $M$ -atoms). 70 pairs of identical accidental atoms  $M$  with the same properties, as other Cu atoms, were placed near the GB, at a distance 2.6 nm from each other, sufficient to exclude interaction between pairs.

The energy of interaction ( $E_p$ ) between the atoms was introduced, as well as the energy of segregation at GB ( $E_s$ ). The mean square displacement of atoms within 100 ns at 1000 and 1200 K was measured. The data on displacement were recalculated to diffusion coefficients by the equation

$$D_b = \sum \frac{dx^2 + dy^2}{4t}. \quad (16)$$

Table 2. GBD coefficient in dependence on interaction energies

Model Number	$E_{pair}$ , eV/atom	$E_{seg}$ , eV/atom	$D_b$ , $m^2/s$	
			1000 K	1200 K
1	-0.059	0.008	$3.94 \cdot 10^{-11}$	$2.19 \cdot 10^{-10}$
2	-0.199	0.006	$2.08 \cdot 10^{-11}$	$1.46 \cdot 10^{-10}$
3	-0.497	0.014	$4.01 \cdot 10^{-12}$	$5.69 \cdot 10^{-11}$
4	-0.063	0.478	$2.06 \cdot 10^{-11}$	$9.47 \cdot 10^{-11}$
5	-0.285	0.463	$5.94 \cdot 10^{-12}$	$4.87 \cdot 10^{-11}$

It is seen that diffusion coefficients decrease with increasing the pair interaction energy and segregation energy.

Such effect comes due to **two different reasons**: *the mobility of complexes* is very low comparing with the single (free) atoms, If the fraction of free  $M$ -atoms decreases, the effective GBD coefficient also decreases.

It is important to underline, that mobility of the free atoms does not change and depends only on temperature.

The **second** reason is related to *distribution of atoms* through adjacent to GB lattice, where mobility, and their contribution to diffusion coefficient are negligible.

It is possible to separate arbitrary the GB region to 3 zones: the central zone “0” with the width 0.065 nm, “1” – the zone of the next 0.08 nm from both sides of the central zone, “2” – the all other space. Evolution of the number of  $M$ -atoms (single and in the complexes with  $i$   $M$ -atoms) is shown on Fig. 8.

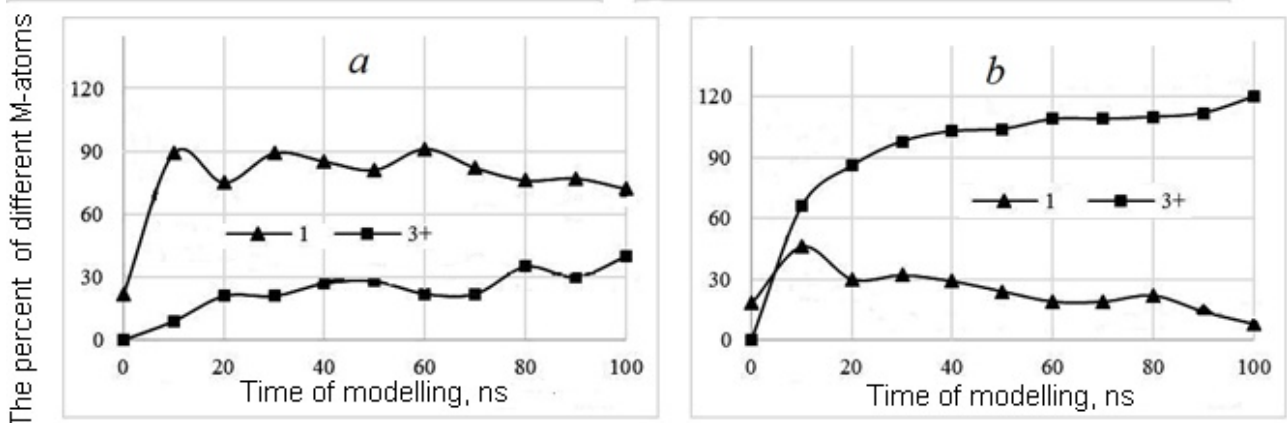


Fig. 8. Evolution of the number of  $M$ -atoms (single and in the complexes with  $i$  marked atoms (1 and 3+) at 1000K  $E_{pair} = -0.2$  eV/atom (a); 1200 K,  $E_{pair} = -0.5$  eV/atom (b).

It is seen that the  $M$ -atoms, originally located in zone “0”, are distributed over the zones and the higher  $E_{pair}$  and lower the temperature, the more  $M$ -atoms are in zone “0”, where they have the highest mobility and vice versa.

The next step is the **energetic distribution** of atoms in GB region. According to Langmuir, the surface is isotropic, i.e. all atoms in GB plane have the same energy. Meanwhile it is evident that in atomic approximation GB cannot be described as isotropic plate. It is necessary to take into account energetic contribution of each atom in GB region. To solve the problem we have to **compare** the energy of system **before and after** displacement atom from **the bulk to the different GB sites**.

**The modeling is as follows.** One atom from the bulk was replaced by the  $M$ -atom. Following, the summary energy of the system was calculated after minimization at 0 K. Comparing energies before and after replacing, we received the energy of every state.

**As the model corresponds to periodic boundary conditions** and contains symmetric boundaries, it is possible to separate the region (Fig. 9). It contains 72 atoms. Translating this region in directions (100) (010) we can obtain all energetic states of atoms in vicinity of GB. Consequently, we can calculate the change of system energy at atom transition from the bulk to this region.

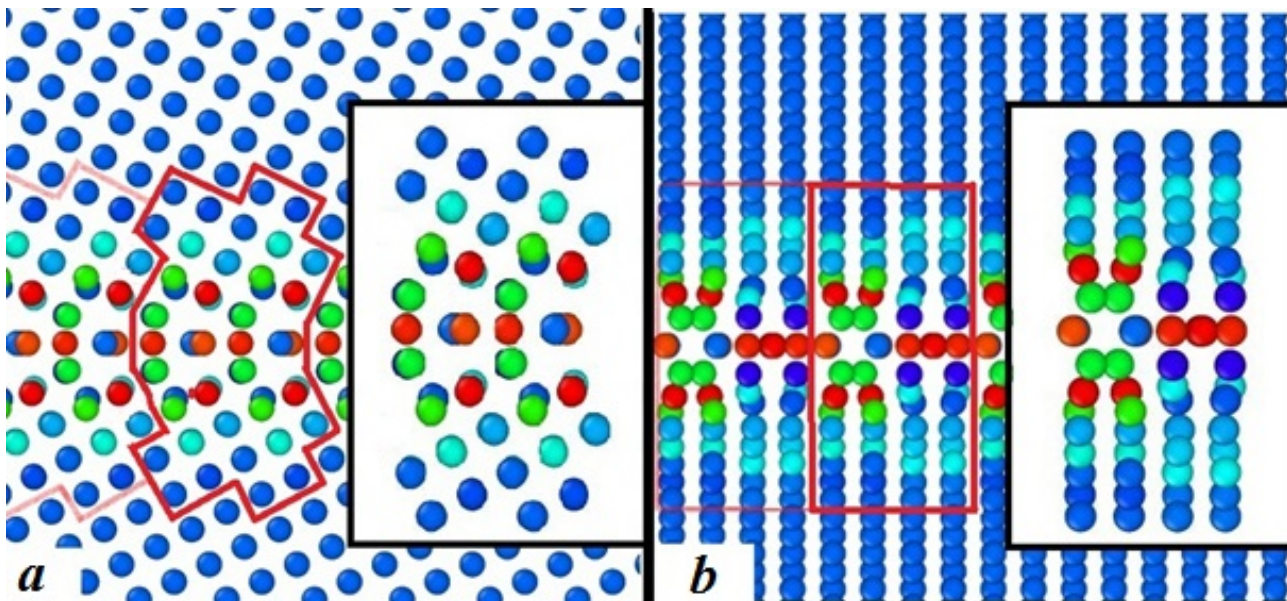


Fig. 9. The translation of this region in directions (100) and (010) permit to describe all energetic states of atoms in GB

We separate the **layers** at which the atoms **group** (Fig. 10) and we calculate dependence of **energy of each atom in the layer** on distance from boundary plane of symmetry (zero layer) – Table 3, Fig 10.

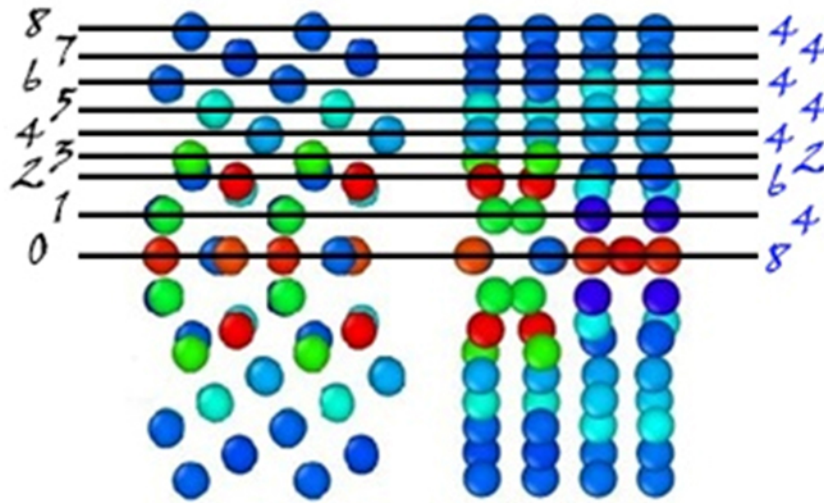


Fig. 10. Distribution of atoms by layers. At the left – the number of layer, at the right – the number of atoms in the layer

Table 3. Atom and segregation energy ( $E_s$ ) of the 0, 1 and 2 layers for the potential 5.  $h$  – distance from the zero layer (in Å)

Layer № 0			Layer № 1			Layer № 2		
Atom number	$h$	$E_s$	Atom number	$h$	$E_s$	Atom number	$h$	$E_s$
17	0.00	$2.23 \cdot 10^{-2}$	18	1.289	$-1.02 \cdot 10^{-1}$	9	2.34	$3.27 \cdot 10^{-1}$
19		$4.30 \cdot 10^{-1}$	22		$-1.02 \cdot 10^{-1}$	12		$2.65 \cdot 10^{-1}$
20		$2.23 \cdot 10^{-2}$	54		$3.56 \cdot 10^{-1}$	14		$2.65 \cdot 10^{-1}$
24		$4.30 \cdot 10^{-1}$	57		$3.56 \cdot 10^{-1}$	16		$3.27 \cdot 10^{-1}$
55		$4.46 \cdot 10^{-1}$				48		$1.22 \cdot 10^{-1}$
56		$-5.78 \cdot 10^{-2}$				51		$1.22 \cdot 10^{-1}$
60		$-5.78 \cdot 10^{-2}$						
61		$4.46 \cdot 10^{-1}$						

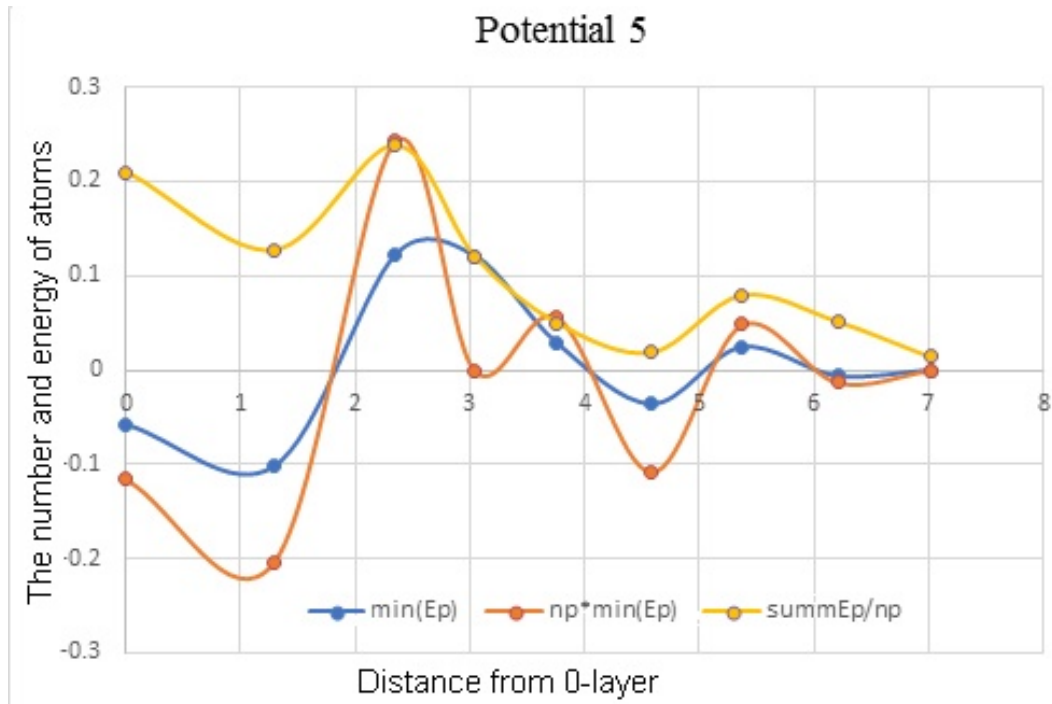


Fig. 11. Distribution of energies in dependence on distance from 0-layer for the potential 5:  $\min(E_p)$  – minimal gain of energy at transition of each  $M$ -atom from the bulk to GB;  $np$  – the number of atoms with such energy in the layer;  $np_{\min}(E_p)$  – summary energy of all sites with minimal energy (capacity of layer);  $\text{summ}(E_p/np)$  – summary gain of energy for the layer divided on the number of atoms  $p_n$  the layer (specific energy of the layer)

From the Table 3 and Fig. 11 it is clearly seen that the energy of the atoms replaced to different sites in different layers is very different. For example the replacing of the atoms to the site 56 and 60 in 0-layer and to the sites 18 and 22 in 1 layer give the gain in energy equal 0.06 and 0.1 eV/atom consequently comparing with the bulk. Remember that the heat energy at 1000 K is approximately 0.1 eV/atom. There are two sites in the 0-layer with the loss of energy 0.02 eV/atom. The other sites in all layers give the loss of energy from 0.4 to 0.1 eV/atom. Beginning from the 4<sup>th</sup> layer there are the sites with the energy less than 0.03 eV/atom comparing with the bulk. In the 8<sup>th</sup> layer the energy does not differ from the bulk.

So, the boundary is significantly non-homogeneous, what may be important for the construction of the adsorption isotherms.

On the Fig. 12 there are only two curves – dependencies of the specific energy on distance from the GB plane (number of the layer) for the potentials 1 (the lower curve) and 5 (the upper curve). The upper curve is linearized. The change of energy between 0 and 8<sup>th</sup> layers is approximately 1.3 eV/atom. It is important to underline is energy dependence on distance from the GB plane (outside the GB), but not inside GB plane.

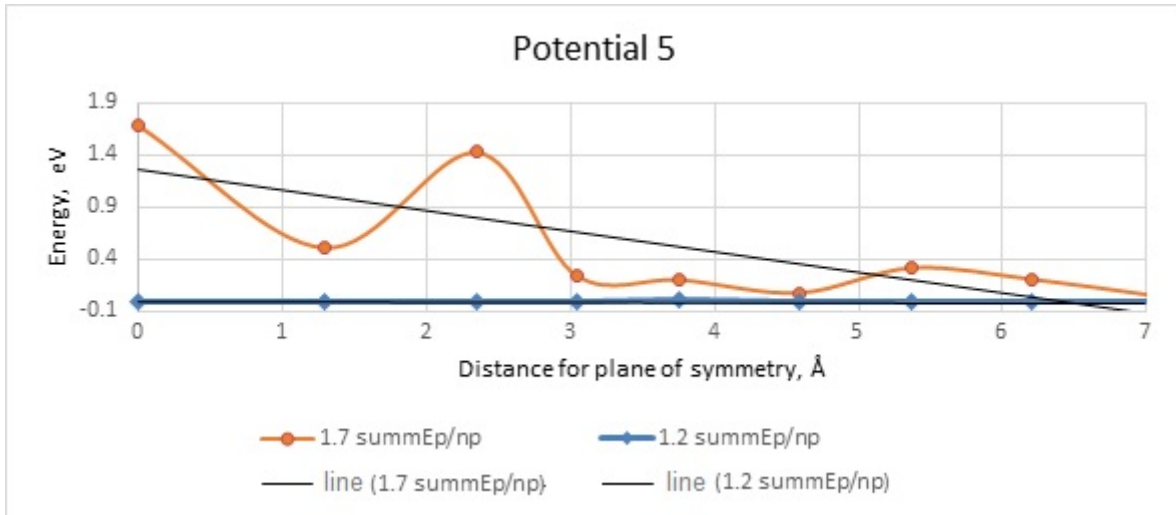


Fig. 12. Dependence of the specific energy on distance from the GB plane (number of the layer) for the potentials 1 (lower curve) and 5 (upper curve)

The data obtained permit to compare the specific energy of the nearest to GB plane layers (0, 1, 2) for different potentials (Table 4).

Table 4 Distribution of the specific energy by 0, 1, 2 layers for different potentials

Potential	0 layer	1 layer	2 layer	$E_p$	$E_s^*$	
1	$-3.8 \cdot 10^{-2}$	$-3.2 \cdot 10^{-2}$	$-3.1 \cdot 10^{-2}$	-0.059	0.008	
2	$2.6 \cdot 10^{-2}$	$-4.6 \cdot 10^{-5}$	$4.5 \cdot 10^{-2}$	-0.199	0.006	
3	$2.1 \cdot 10^{-1}$	$1.3 \cdot 10^{-1}$	$2.4 \cdot 10^{-1}$	-0.497	0.014	
4	$3.4 \cdot 10^{-1}$	$2.4 \cdot 10^{-1}$	$1.6 \cdot 10^{-1}$	-0.063	0.478	
5	$3.4 \cdot 10^{-1}$	$2.2 \cdot 10^{-1}$	$2.0 \cdot 10^{-1}$	-0.283	0.463	

One can see that in absence of the pair interaction energy and segregation energy (potential 1) summary energy of 0, 1, 2 layers is slightly negative. All interactions lead to the positive value. Comparison of the potentials 3 and 4 shows that  $E_s$  (desorption energy) leads in 0.1 layers to stronger effect than negative pair energy. At 2 layer the effect is nearer. It seems that the influence of the pair energy is weaker than segregation effect.

### Summary

Some aspects of grain boundary segregation (GBS) are discussed. This paper adds two new sprouts. The first is connected with atomic interaction, formation of atomic complexes in boundary region and delay of GBD. The second – with nonhomogeneity of energy distribution between boundary sites.

Molecular dynamics (MD) simulation was fulfilled with the EAM potential for pure Cu and for binary Cu-M solution, where M is a second component with the same characteristics as for a pure Cu, but with addition of two energies: pair interaction and segregation energy. It was shown the effect of complexes formation and also that complexes decrease GBD coefficient of M-atoms due to two different reasons.

The first reason is connected with a small complexes mobility comparing with a “free” atoms. As a result, a fraction of free atoms decreases and the effective GBD coefficient also decreases.

The next reason is connected with the transition of the part of solute atoms from GB to the adjacent lattice, where their mobility is negligibly small comparing with the atoms in GB plane. of symmetry. The “free” atoms move exactly with the same mobility as in the absence of complexes (in a pure Cu). It means that decrease of GBD coefficient is connected with the number of mobile

atoms but not their mobility.

The second new point is connected with analysis of atomic distribution through the sites in GB. with different energy. It was necessary to consider a contribution of each atom in GB. The GB region was divided on the layers. The distribution was received in dependence on layer distance from GB plane of symmetry and on two above mentioned additive energies.

**Acknowledgements.** This work was done under support of RFBR-grant #20-03-00387. Authors are grateful to Dr. L. Klinger for fruitful discussions.

## References

1. H.G. Gleiter, B. Chalmers. High-Angle Grain Boundaries. Pergamon Press, 1972.
2. B.S. Bokstein, Ch.V. Kopetckii, L.S. Shvindlerman. Thermodynamics and Kinetics of Grain Boundary in Metals. Moscow, Metallurgiya, 1986 (in Russian).
3. G Gottstein, L. Shvindlerman. Grain Boundary Migration in Metals. CRC Press. 2010. 682 p.
4. I. Kaur, Y. Mishin and W. Gust: Fundamentals of Grain and Interphase Boundary Diffusion, Wiley, Chichester (1995).
5. P. Lejcek and S. Hofmann. Critical Reviews in Solid State and Materials Science, 20 (1), (1995), 1.
6. Y. Mishin et al. Acta Materialia, V. 58 (2010), p. 1117.
7. B. Bokstein and A. Rodin. Grain Boundary Diffusion and Grain Boundary Segregation in Metals and Alloys. Diffusion Foundations Vol. 1 (2014) pp. 99-122.
8. B.S. Bokstein, M.I. Mendeleev, D.J. Srolovitz, Thermodynamics and Kinetics in Materials Science. Oxford Univ. Press, 2005.
9. E.W. Hart in the Nature and Behaviour of Grain Boundaries (H.Hu, ed.) Plenum Press, N.-Y., 1982.
10. J.W. Gibbs. The collected Works in two Volumes. Longmans, Green and Co, N.-Y., 1928.
11. G. Martin and B. Perrillon: in "Grain Boundary Structure and Kinetics" Metals Park, OH: Amer. Soc. Metals, (1980) p. 239.
12. B.S. Bokstein, V.E. Fradkov and D.L. Beke: Phil. Mag., V. 65 A, N 2, (1992) p. 277.
13. Y. Mishin and Chr. Herzig: J. Appl. Phys., V. 76 (1993) p. 8206.
14. M. Temkin: Russ. J. of Phys. Chemistry, V.15 (1941) p. 296.
15. R.M. Fowler and E.A. Guggenheim. Statistical Thermodynamics, Cambridge, (1939).
16. M. Guttman. Surface science, vol 53 (1975) pp. 213-217.
17. R.P. Messmer and C.L. Briant. The role of chemical bonding in grain boundary embrittlement. Acta metall., vol. 30, pp. 457-467, 1982.
18. J. Bernardini and P. Gas. Diffusion and 2D Chemistry in Grain Boundaries, Def. and Dif. Forum 95-98 (1993) 393-404.
19. B.S. Bokstein, A.O. Rodin, A.N. Smirnov. Thermodynamics of grain boundary adsorption in binary systems with limited solubility. Zt. fur Metkunde, 10 (2005) 1094-1099.
20. B. Bokstein, A. Rodin. Concentration phase transition associated with grain boundary segregation in systems with restricted solubility. Intern. Journal of Mater. Research 4 (2009) 522-524.
21. B.S. Bokstein, V.A. Esin, A.O. Rodin. New model of grain boundary segregation with formation atomic complexes n boundary. FMM. 109(4) (2010) 1-4 (in Russian).
22. M.I. Mendeleev, A.O. Rodin, B.S. Bokstein. Computer simulation of Fe diffusion in liquid Al and along Al grain boundaries. Def. and Dif. Forum, 309-310 (2011). pp. 223-230.
23. A. Itckovich, M. Mendeleev, A. Rodin and B. Bokstein. Computer modeling of atomic clusters formation in grain boundaries. Rev. Adv. Mater. Sci. 52, № 1/2 (2017), pp.1-4.
24. B.S. Bokstein, A.O. Rodin, A.A. Itckovich. History and Modern State of Grain Boundary Segregation Problem and Its Effect on Grain Boundary Diffusion. Def. and Dif. Forum (2019) in press.